



# Comparative Study of the Fractured Humerus Fixation by Intramedullary Nailing and Compression Plate

Ibrahim Keddar · Benaoumeur Aour · Samir Zahaf

Submitted: 1 February 2022 / in revised form: 21 July 2022 / Accepted: 17 August 2022 / Published online: 2 October 2022  
© ASM International 2022

**Abstract** Comminuted humeral fractures are usually treated with locking plates or intramedullary nails with satisfactory clinical results. It is important to note that the success of this type of implantation depends on the long-term stability, adaptability and integration of the humeral bone tissue while maintaining a lesser and optimal pressure distribution in the surrounding bone. In this context, the main objective of the present work is to search for rational solutions to reduce and minimize stress concentrations by comparing the fractured humerus fixation using intramedullary nailing and a compression plate. To this end, these implants were designed and implanted in a fractured humerus and analyzed by finite elements using three different types of loadings (axial force, inclined force, and torsional moment). To assess the biomechanical behavior of the different implants, the distributions of von Mises stresses, strains and total displacements in the implants and bones (cortical and cancellous) of the humerus were compared. The numerical results obtained showed that the fixation systems by a locking plate or an intramedullary nail fixed by six screws played a very important role in the absorption and minimization of the stresses, and consequently, the stabilization of the surgical treatment adopted. Indeed, the nailing system gives a lower level of von Mises stress and strain in the cortical and cancellous bone of the

humerus compared to the plate model under the influence of axial forces and torques, whereas the compression plate shows the lowest values of stresses and strains in the bone when the applied load is of the inclined force type.

**Keywords** Fracture · Humerus · Von Mises stress–strain · Intramedullary nailing · Cortical bone · Spongy bone · Plate surgical treatments · Finite element method

## Introduction

Among the most frequent injuries, that of the proximal humerus fractures is one of the types often encountered in the elderly, with a frequency constantly increasing following the aging of people and the predominance of osteoporosis [1, 2]. Surgical treatment is necessary for the management of this type of fragile failure to obtain and preserve anatomical rehabilitation, allows precocious functional resumption, and guarantees fast healing. Treatment options for joint preservation consist of compression plate and intramedullary nailing. The insertion of fixation plates has revolutionized the handling of fractures at this anatomical emplacement [3, 4]. Though, the complications rate linked to fixation in brittle bone, considering also intra-articular screw punching and reduction loss, remains great, reaching up to 36% in the overall population and up to 86% for the greatest at-risk mental population [3–8]. Surgical treatment of proximal humerus fractures in the setting of osteoporosis is especially difficult because of insufficient bone support, complicated loading conditions of the shoulder complex, fragmentation, and restricted surgical intervention [9]. This challenge, in combination with the high degree of complications, requires well-established

---

I. Keddar · B. Aour  
Laboratory of Applied Biomechanics and Biomaterials (LABAB), Department of Mechanical Engineering, National Polytechnic School of Oran, BP 1523 El Mnaour, Oran, MA, Algeria

S. Zahaf (✉)  
Department of Technology, University of Djilali Bounama – Khamis Meliana, Ain Defla, Algeria  
e-mail: zahafsamir1983@gmail.com

methodologies for osteosynthesis and preoperative planning using more convenient and perfect design techniques.

Difficulties encountered during in vitro biomechanical experimental testing limit the reliability of each technique and, therefore, the conception procedure. On the other hand, the robustness of numerical modeling has been recognized by several authors in the prediction of the biomechanical quality of bones [10] and the reliability evaluation of osteosynthesis devices [11]. Very limited numerical investigations have studied the difficulties of proximal humeral fractures treatment, by comparing the results obtained by different types of implants [12, 13], by studying the influence of the locking screw geometry [14], by studying the biomechanical behavior of the bone cement [15] and by studying the fracture gap dimension [16]. Though, these models were generally developed based on simple boundary and loading conditions and using a single sample. The studies were limited to the assessment of the elastic rigidity and the stress distribution in the implant and the bone but did not consider the prediction of the failure of the adopted solution [17].

It has recently been shown that finite element modeling (FEM) can predict the failure of the experimental cyclic concept of proximal humerus fracture fixation with locking plates [18]. Nevertheless, the development of these models and the obtaining of reliable results require considerable time and significant user interactivity. Automating these simulation phases could effectively help the implant delivery process by supplying fast feedback on bio-physico-mechanical reliabilities. Furthermore, there are very few studies that have considered the implant design, loading conditions, diversity of complex regimes, variations in bone grade and bone failure type [17].

Therefore, there remains a need for numerical tests and skillful research through numerical models that would consider the spectrum of complicated conditions and would provide effective estimates related to individual measurements to elucidate the steps of success by means of a parametric evaluation.

**Fig. 1** Bones of the humerus shown in Design Modeler (Ansys): (a) cancellous bone; (b) cortical bone containing six holes for fixation screws

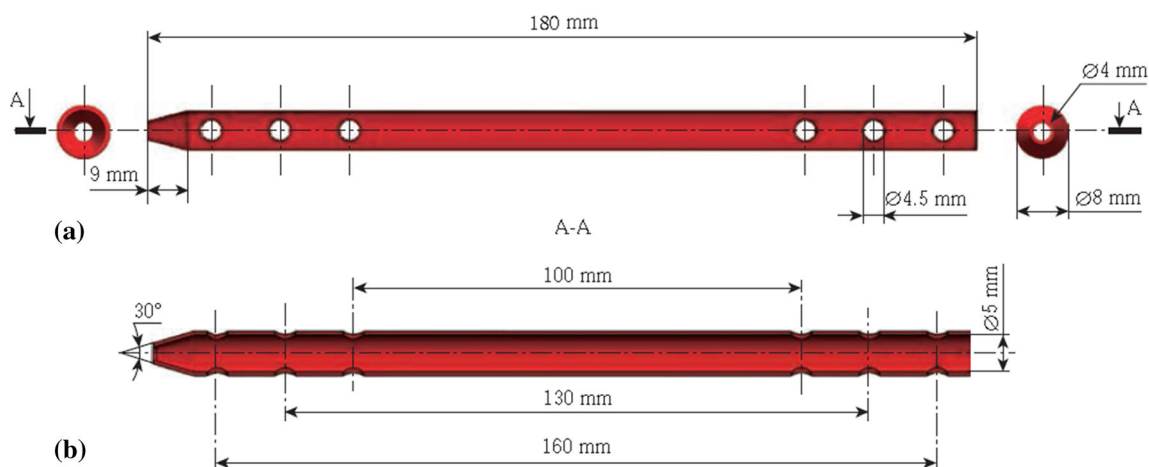


**Fig. 2** Illustration of the intramedullary nail made using SolidWorks: (a) front view, and (b) cross-sectional view A-A

**Fig. 3** Definition drawing of the plate fixation system

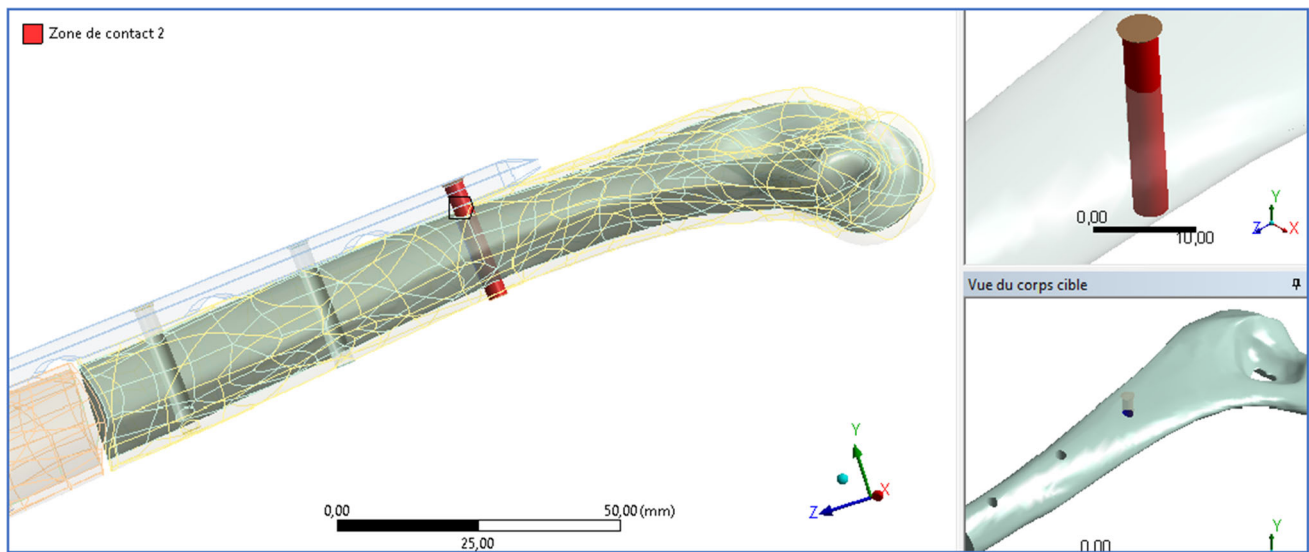
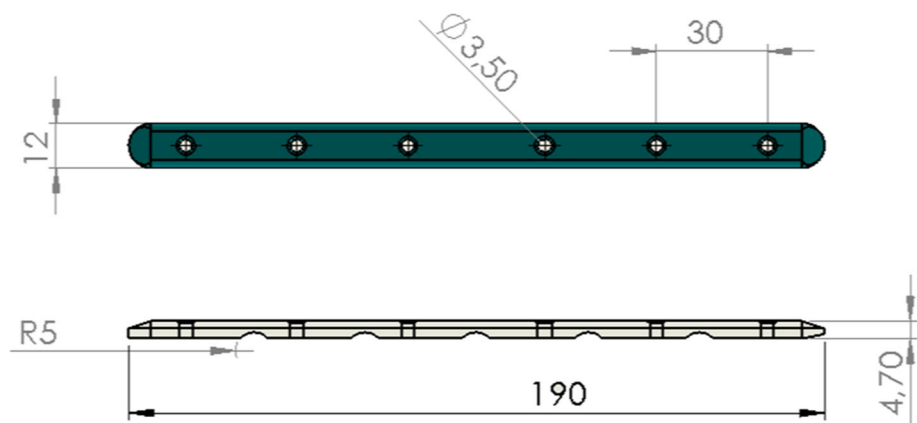


**Fig. 4** Illustration of screw-plate-bone contacts is defined as fully fixed

### Geometric Modeling

Plates are used if there was a risk of rotation that would shift the axis of the underlying joints, or for short bones. There are a variety of plates and screws of suitable shapes, allowing all of these to be fixed in the correct position. The numerical models developed for this study consist of four main parts. The cortical and cancellous bone (Fig. 1) which are obtained using the segmentation and 3D reconstruction techniques described in our previous paper [19]. The intramedullary nail and locking plate fixation systems were designed using Solidworks software (Figs. 2 and 3).

### Finite Element Modeling

The aim of this finite element modeling is to study the stresses and strains distributions in the various components of nail and plate fixation systems, including cortical and

cancellous bone under different types of loading. The numerical simulations were performed using ANSYS Workbench software. The biomaterials properties, the boundary conditions and the meshing of the models will be presented in detail in this section.

### Biomaterials' Properties

For the finite element analysis of the developed models, we need to introduce the mechanical properties of each component. In this study, we considered isotropic, elastic, and linear behavior. The Young's moduli of cancellous and cortical bone are, respectively, 1,380 MPa and 13,800 MPa with a Poisson's ratio of 0.3 [19]. The contact interfaces between the plate locking screw and the bone were assumed to be completely bonded (Fig. 4). All the elements of the models studied were assumed deformable elements. The materials investigated in the fixtures for the locking plate and the screws were titanium alloy (Ti6-Al4-

**Table 1** Mechanical properties of the model’s components [19–21]

No	Component	Young’s modulus (MPa)	Poisson’s ratio
1	Cortical bone	13,800	0.3
2	Cancellous bone	1,380	0.3
3	Intramedullary nail	110,000	0.33
3	Fixation plate	110,000	0.33
4	Screw	110,000	0.33

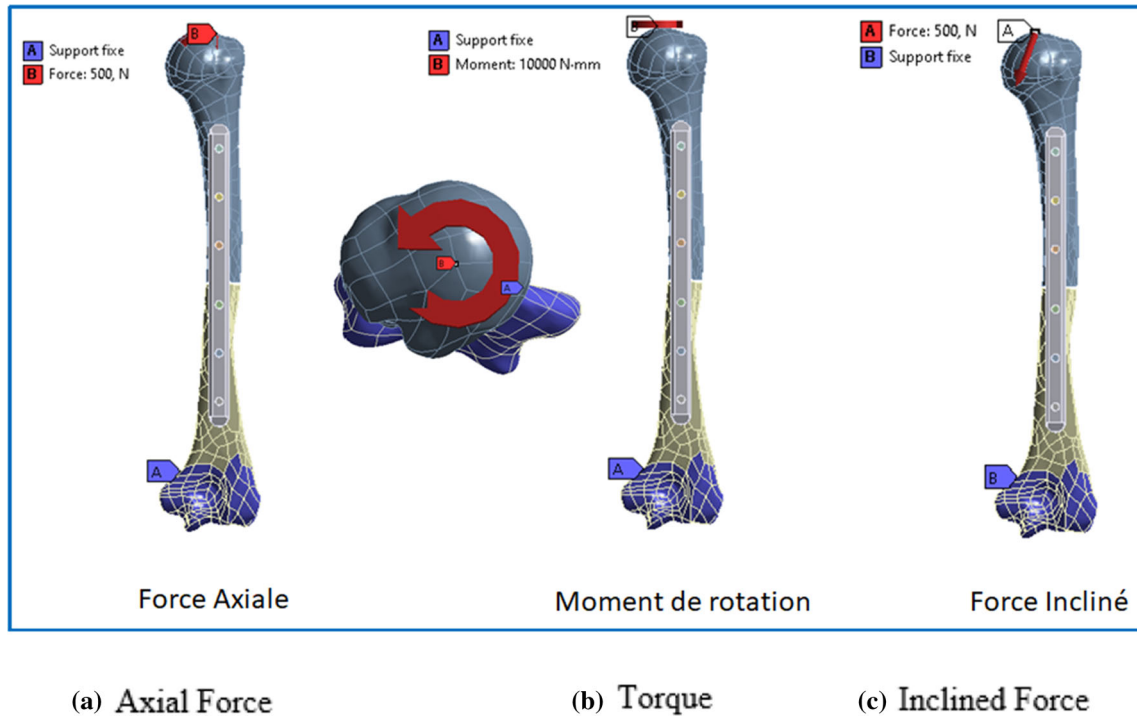


**Fig. 5** Illustration of the boundary conditions used: Fixation of the distal part of the humeral shaft and application of (a) axial force, (b) torque and (c) inclined force on the humeral head

**Table 2** Different types of loads applied to the humeral head

	Load 1	Load 2	Load 3
Force	Axial Force	Inclined Force at 20°	Torque
Value	500 N	500 N	10 Nm
Application points	The humeral head	The humeral head	The humeral head
Embedding	The humeral shaft	The humeral shaft	The humeral shaft

V) with a Young’s modulus of 110,000 MPa and a Poisson’s ratio of 0.33 (Table 1).

**Boundary and Loading Conditions**

Indeed, it is difficult to give actual boundary conditions from real bone locations due to the complex structure of the

human body. Based on the literature [22–24], in this study, we fixed the distal segment of the humeral shaft. Axial force, shear force and torque were applied to the developed models. For the axial force, we applied a load of 500 N oriented vertically in the coronal and sagittal planes to the proximal humeral head. Based on the axial conditions, the angle of the model was changed by 20° to simulate the

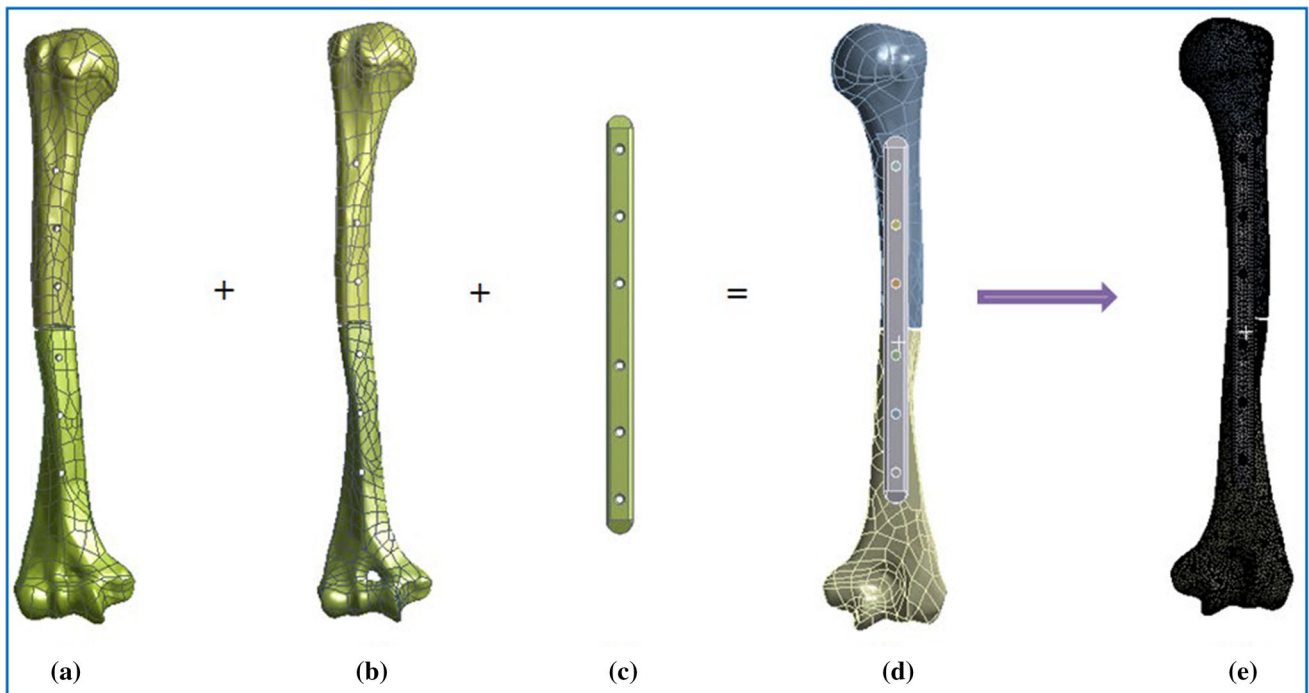
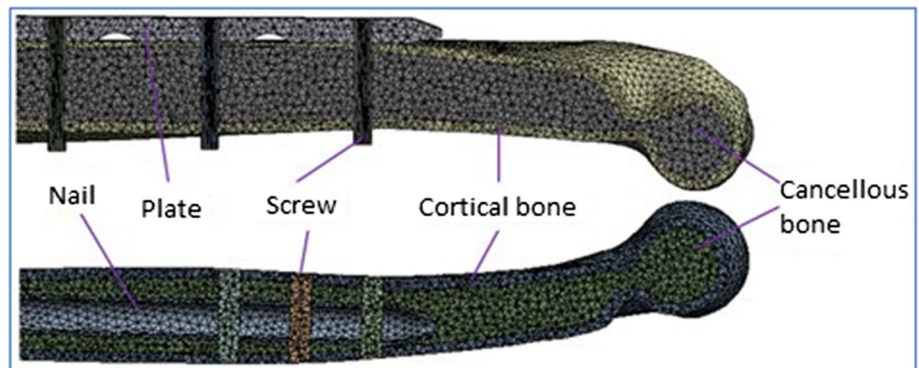


**Fig. 6** The components of the model: (a) cortical bone, (b) cancellous bone, (c) compression plate, (d) assembled model and (e) refined mesh of the model

**Fig. 7** Longitudinal section illustrating the meshes of the different components of the studied models



shear force. The latter simulates the force experienced by a proximal fracture site as the patient leaves a seat or pushes on a cane. To model the rotation, the proximal humeral head is subjected to a torque of 10 Nm applied around the axis of the humeral diaphysis (Fig. 5). All the applied loads are shown in Table 2.

### Models Meshing

The components of the studied models were meshed using 10-node tetrahedral linear elements. The full model of the humerus and compression plate with the six screws includes 283,175 elements and 582,467 nodes (Fig. 6). The

**Fig. 8** (a) Application of the boundary conditions and (b) the mesh used for the numerical validation model in intramedullary nail and plate fixation

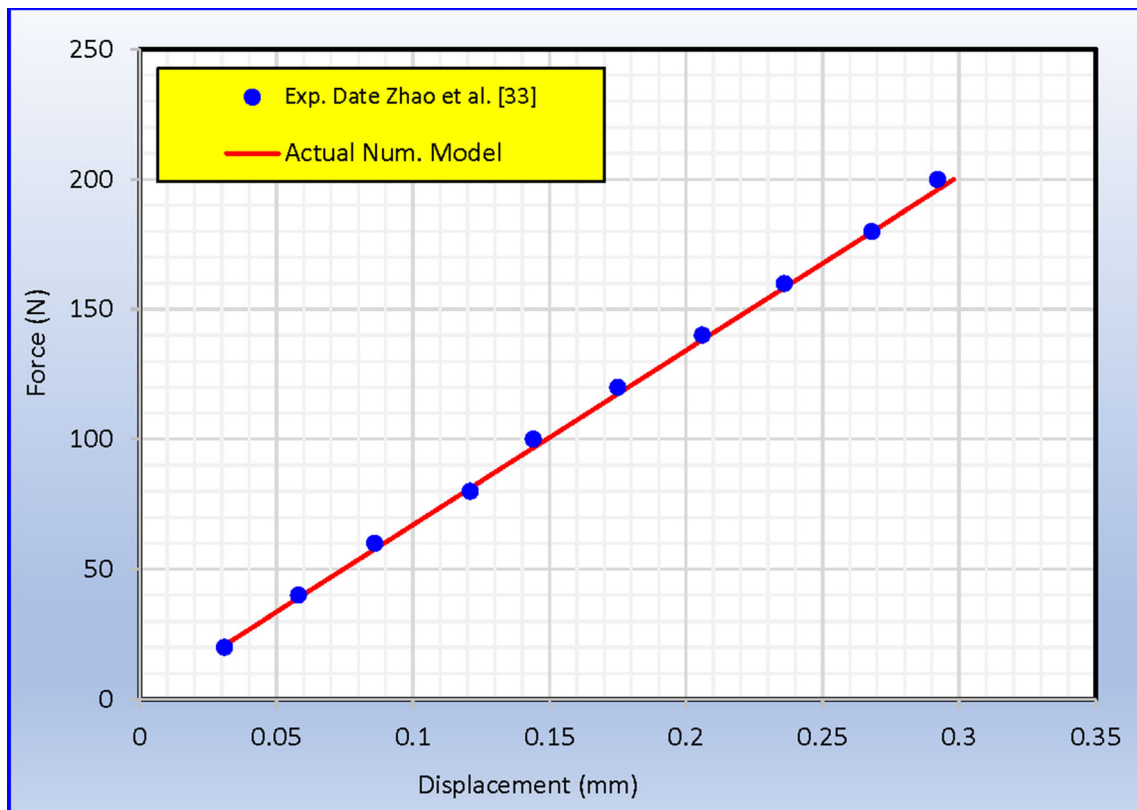
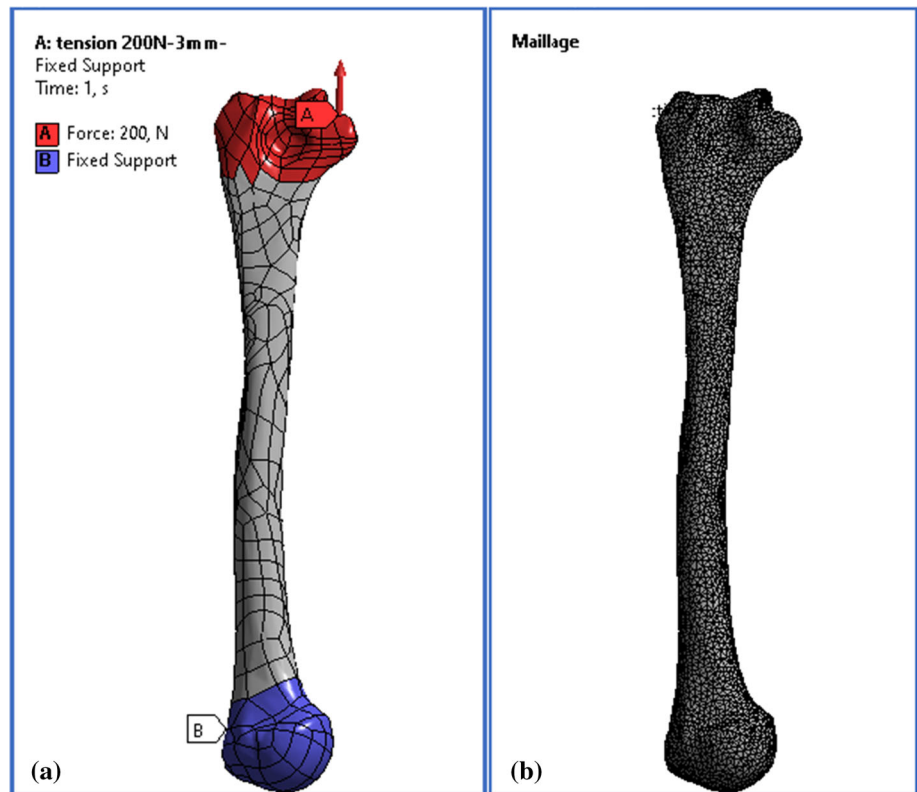


**Fig. 9** Comparison of force–displacement results obtained by the actual numerical simulation with the experimental data given by Zhao et al. [3]

### Intramedullary nail fixation system

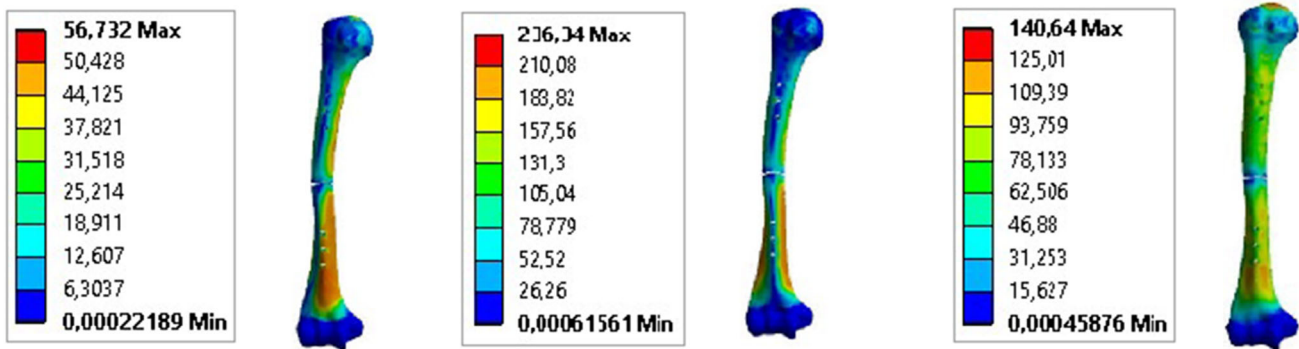


### Plate system for surgical treatments

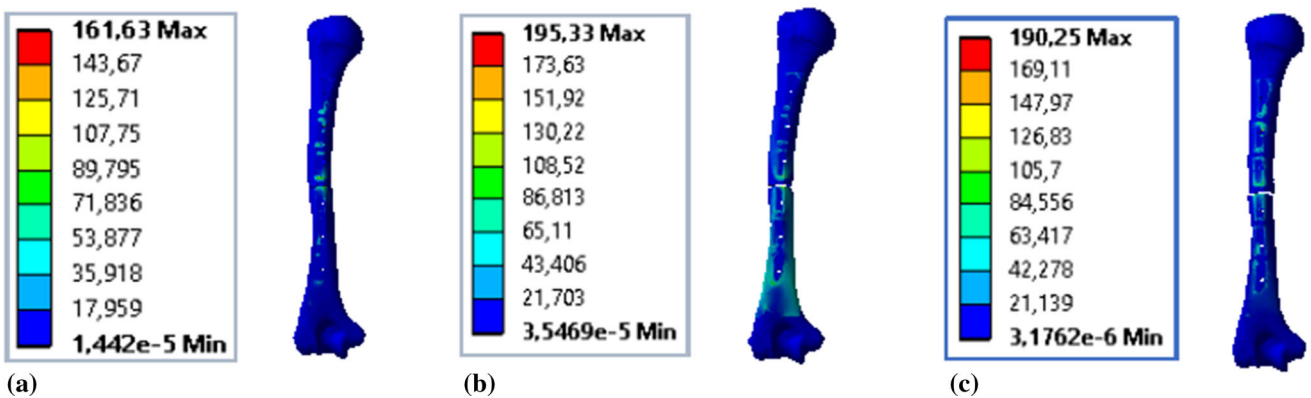


**Fig. 10** Distributions of von Mises stresses in the cortical bone of the fractured humerus for both models (intramedullary nail and plate surgical treatments) for the three types of loadings: (a) axial force, (b) inclined force and (c) torque

cortical and cancellous bones were modeled with tetrahedral elements using (85,220 elements and 150,599 nodes) and (136,086 elements and 199,802 nodes), respectively. The plate and fixation screws were also modeled using tetrahedral elements (61,869 elements and 232,066 nodes). The humerus with the six-screw nailing system was composed of 268,255 elements and 472,882 nodes. The intermediate surfaces between the various constituents of the nailing and compression plate devices were treated as perfectly bonded (Fig. 7).

#### Model Validation

Prior to performing the simulation calculations of the behavior of the fractured humerus fixed by both fixation systems, a validation was performed of the numerical model using an intact humerus in tension whose experimental results are given by Zhao et al. [23]. These are tensile tests under the action of progressive forces applied in steps on the surface of the elbow joint to simulate lifting heavy objects, with the surface of the glenohumeral joint fixed. The applied force varies from 20 to 200 N (with a

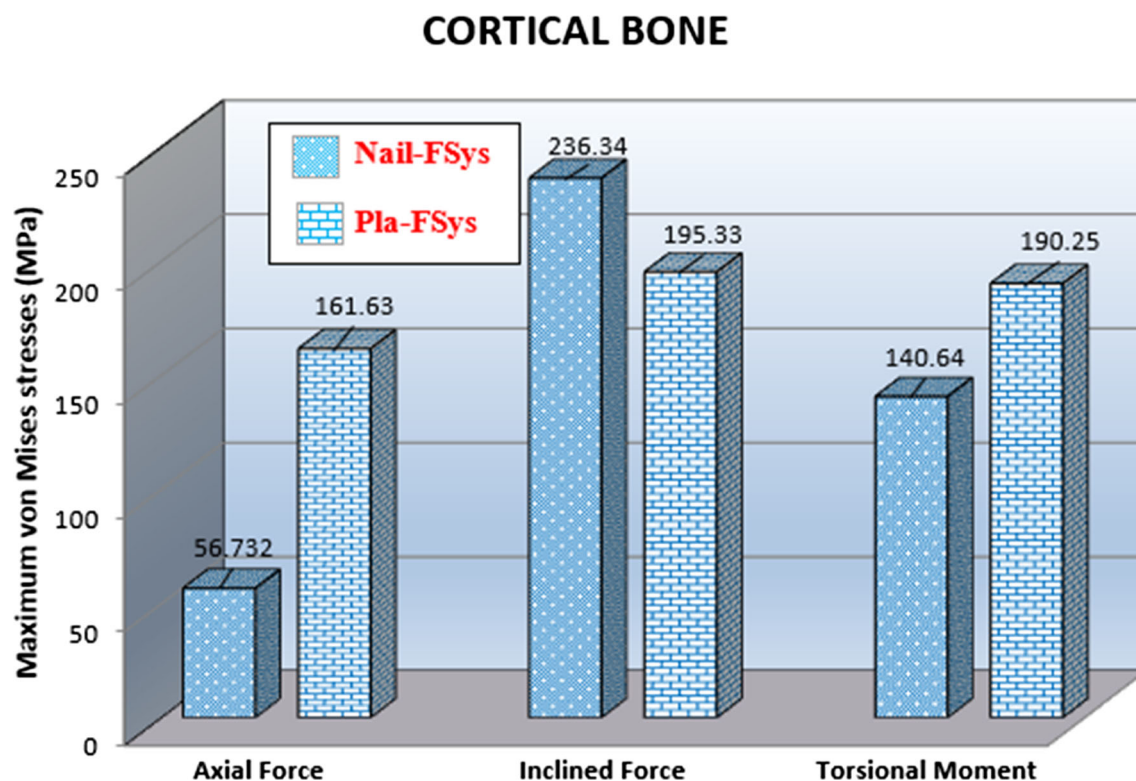


**Fig. 11** Histogram of maximum von Mises stresses in the cortical bone of the fractured humerus for both fixation systems (intramedullary nail and plate fixation system) under the effect of the three types of loads (axial force, inclined force, and torsional moment)

20 N step). These experimental conditions have been reproduced in the finite element code by applying an embedding on the proximal end of the humerus (the humeral head) and a tensile force on the elbow (Fig. 8a). A linear elastic isotropic mechanical behavior was considered with a Poisson's ratio of 0.3 and Young's moduli of 13,400 and 2000 MPa for the cortical and cancellous bones, respectively [23]. A mesh with 10-node tetrahedral elements of size 3 mm was used (Fig. 8b). The comparison of the numerical and experimental results of the force evolution as a function of the displacement is presented in Fig. 9. The results obtained by the developed numerical model using the selected mesh are in good agreement with those obtained experimentally by Zhao et al. [23].

## Results and Discussion

### Distribution of Stresses in the Cortical Bone

Figure 10 shows the distribution of von Mises stresses in the cortical bone of the fractured humerus using both fixation systems (intramedullary nail and plate surgical treatments) for the three types of loading (axial force, inclined force, and torque). The highest level of stress is obtained when using intramedullary nail fixation system under inclined force loading, while the lowest level of stress is obtained in the case of axial force using the same fixation system. Furthermore, it can be observed that the stress concentration is in the lower part of the humerus (see red color in Fig. 10).



### Intramedullary nail fixation system

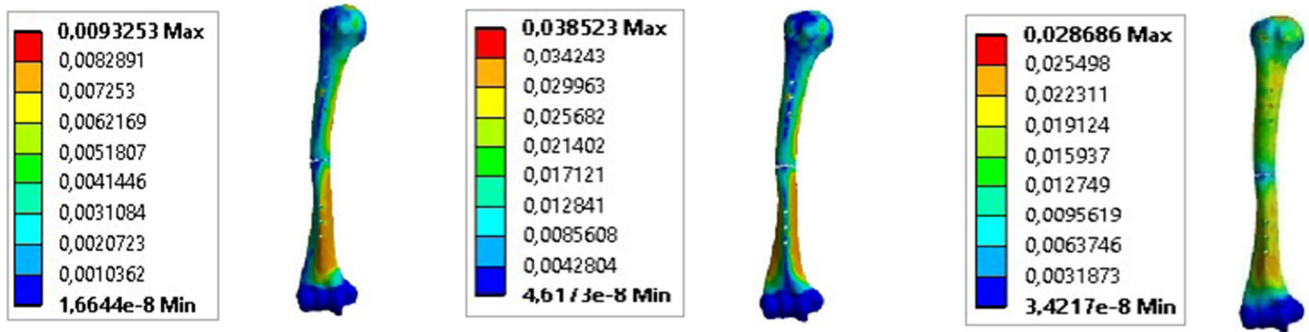


### Plate system for surgical treatments

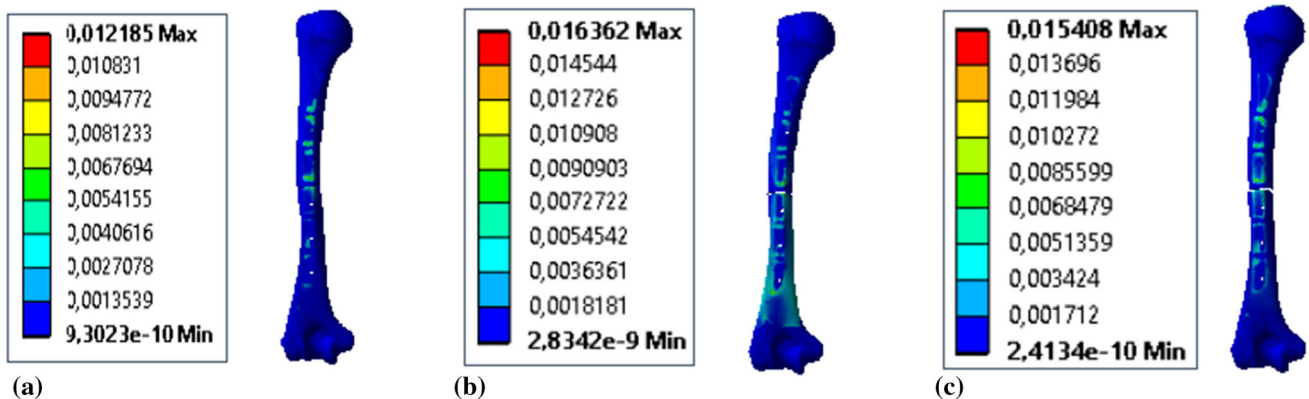


**Fig. 12** Distributions of equivalent strains in the cortical bone of the fractured humerus for both models (intramedullary nail and plate fixation system) for the three types of loadings: (a) axial force, (b) inclined force and (c) torsional moment

Figure 11 shows the evolution of the maximum von Mises stress values in the cortical bone of the fractured humerus using both fixation systems (intramedullary nail and plate surgical treatments) and for the three types of loading. From this figure, the system that generates the most stress in the bone is that of the compression plate. Indeed, in the case of axial force and torsional moment, the maximum stress in the plate system for surgical treatments is always higher than that obtained by intramedullary nail

fixation system. A slight difference was observed between both fixation systems for the case of inclined force. The greatest difference was found in the case of axial force, where it was almost three times that generated by nailing. In general, implantation of the intramedullary nail fixed with six screws results in an equivalent stresses reduction in the cortical bone of the fractured humerus compared to the plate fixation system.

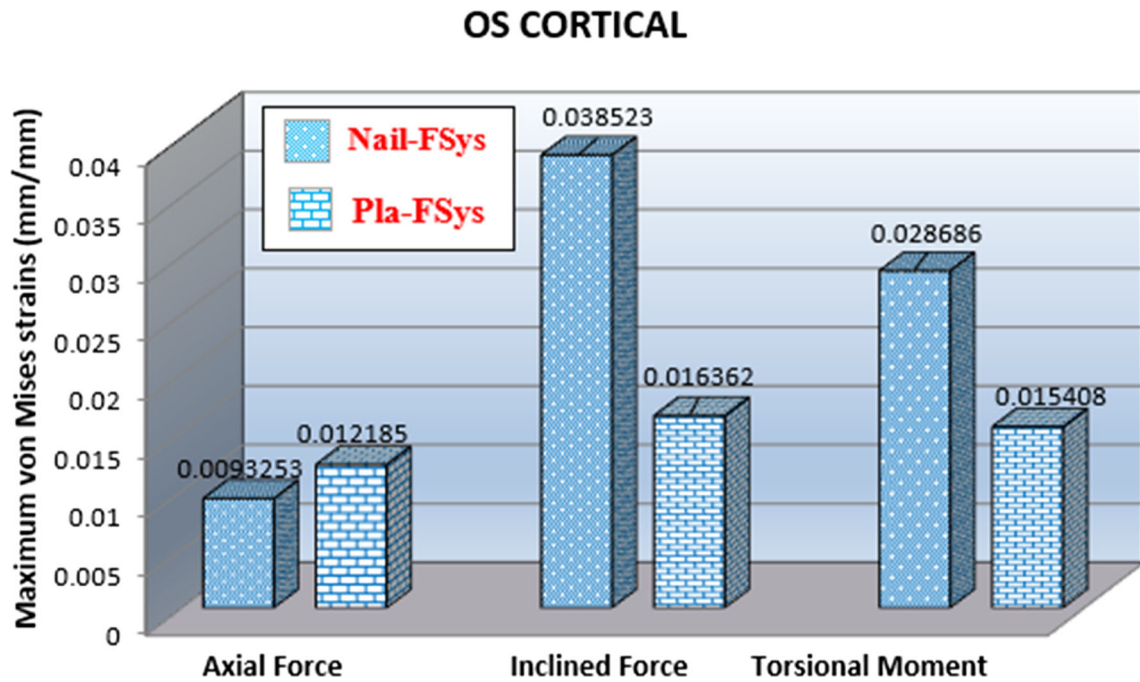


**Fig. 13** Histogram of maximum strains in the cortical bone of the fractured humerus for both fixation systems (intramedullary nail and plate fixation system) under the effect of three types of loading (axial force, inclined force, and torsional moment)

### Intramedullary nail fixation system

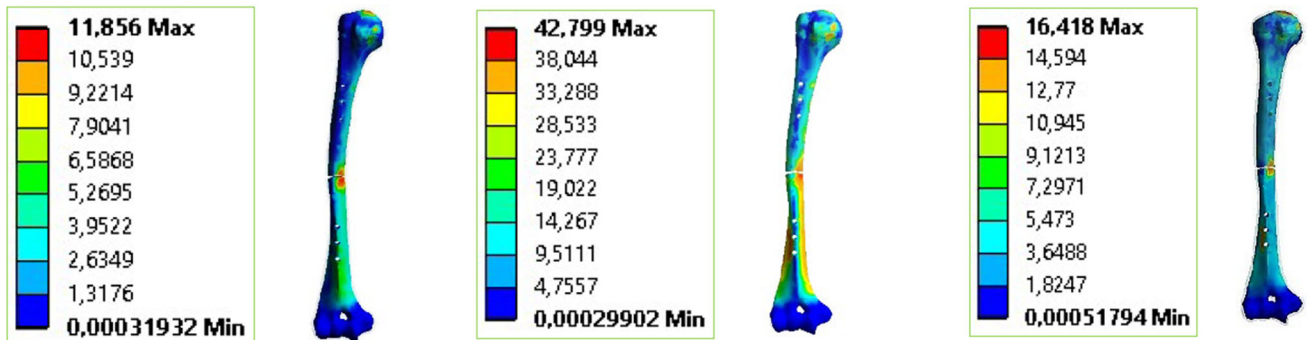


### Plate system for surgical treatments

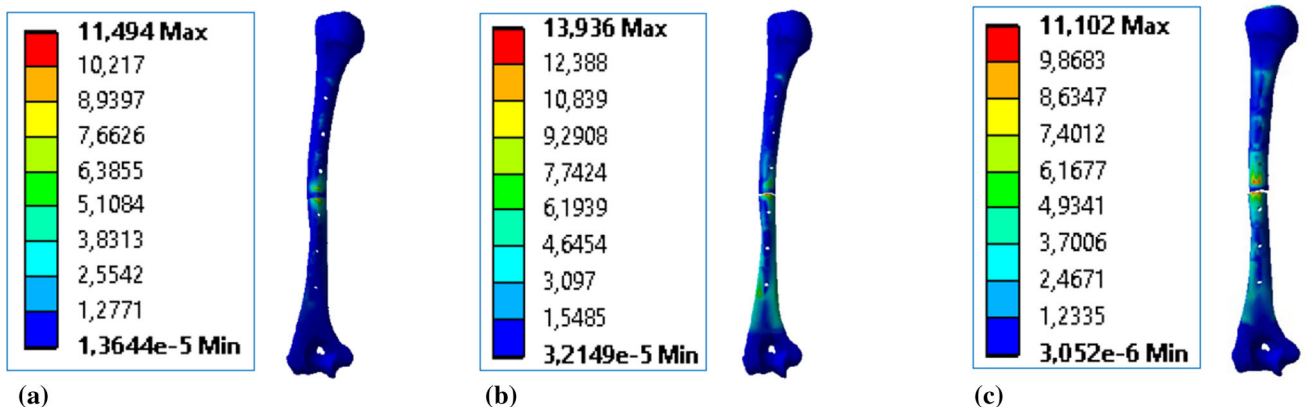


**Fig. 14** Distribution of von Mises stresses in the cancellous bone of the fractured humerus for both models (intramedullary nail and plate fixation system) under the effect of three different loads: (a) axial force, (b) inclined force and (c) torsional moment

### CANCELLOUS BONE

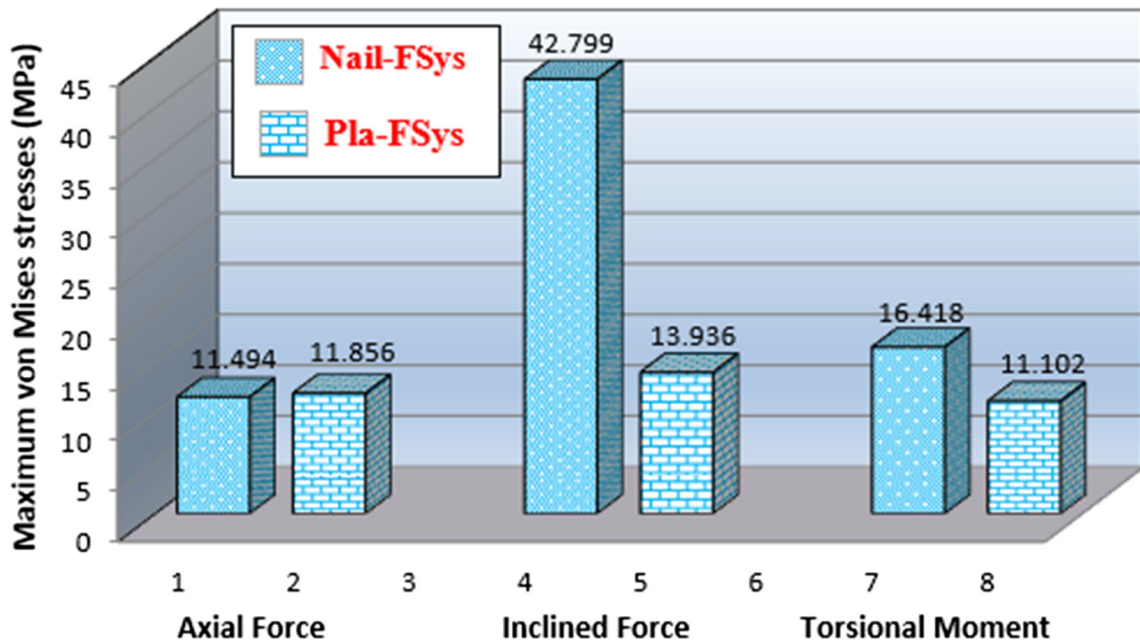


**Fig. 15** Histogram of the maximum von Mises stresses in the cancellous bone of the fractured humerus for both fixation systems (intramedullary nail and plate fixation system) under the effect of different types of loadings (axial force, inclined force and torsional moment)

#### Distribution of Strains in the Cortical Bone

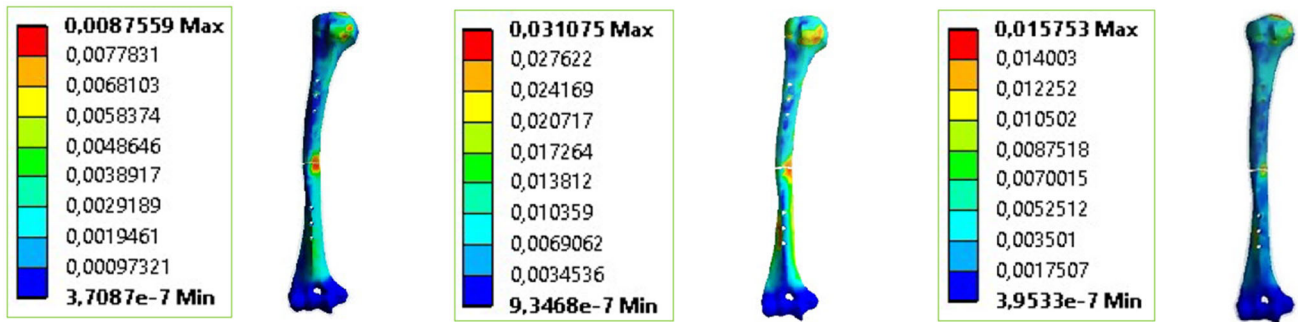
Figures 12 and 13 show, respectively, the strains distribution and maximum strain values in the cortical bone of the fractured humerus using both fixation systems (intramedullary nail and plate surgical treatments) for different types of loadings (axial force, inclined force and torque). The greatest strain is obtained when using the nailing fixation system (Nail-FSys) under the effect of an inclined force loading, whereas the lowest strain is obtained in the case of an axial force using the same fixation system. Furthermore, it can be observed that the maximum strains obtained in the case of the nailing fixation system (Nail-FSys) are almost twice of those obtained by compression plate when the applied loads are inclined forces or torsional moments (Fig. 13). A slight difference

was found between both fixation systems when the applied load is an axial force.

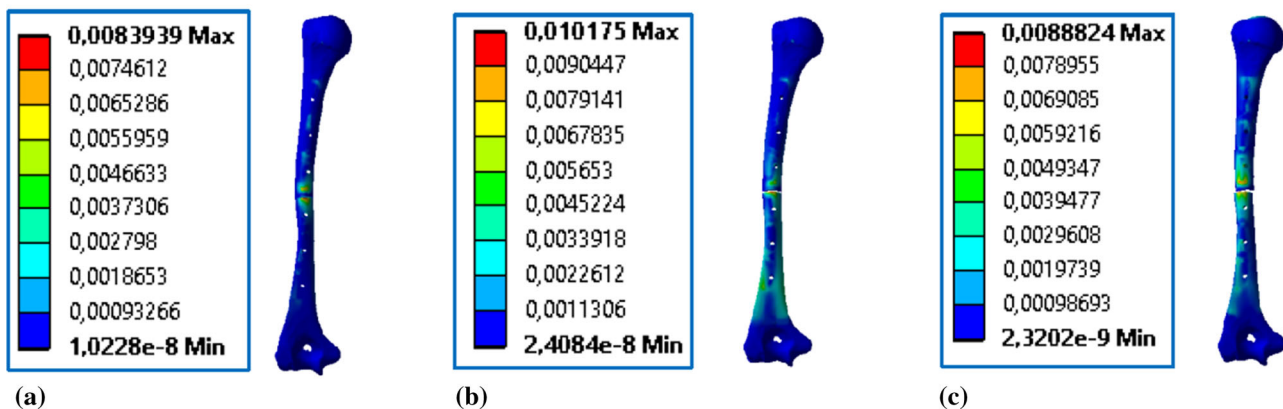
#### Distribution of von Mises Stresses in the Cancellous Bone

Figure 14 shows the distribution of von Mises stresses in the cancellous bone of the fractured humerus using both fixation systems (intramedullary nail and plate fixation system) for the three types of loading (axial force, inclined force, and torsional moment). The highest stress level is obtained when using the nailing fixation system (Nail-FSys) under the effect of an inclined force loading, while the lowest stress level is obtained under torsional moment using the second fixation system (Pla-FSys). Furthermore, it can be observed that the stress concentration is in the

## Intramedullary nail fixation system



## Plate system for surgical treatments



**Fig. 16** Distribution of von Mises strains in the cancellous bone of the fractured humerus for both models (intramedullary nail and plate fixation system) under different types of loading: (a) axial force, (b) inclined force and (c) torsional moment

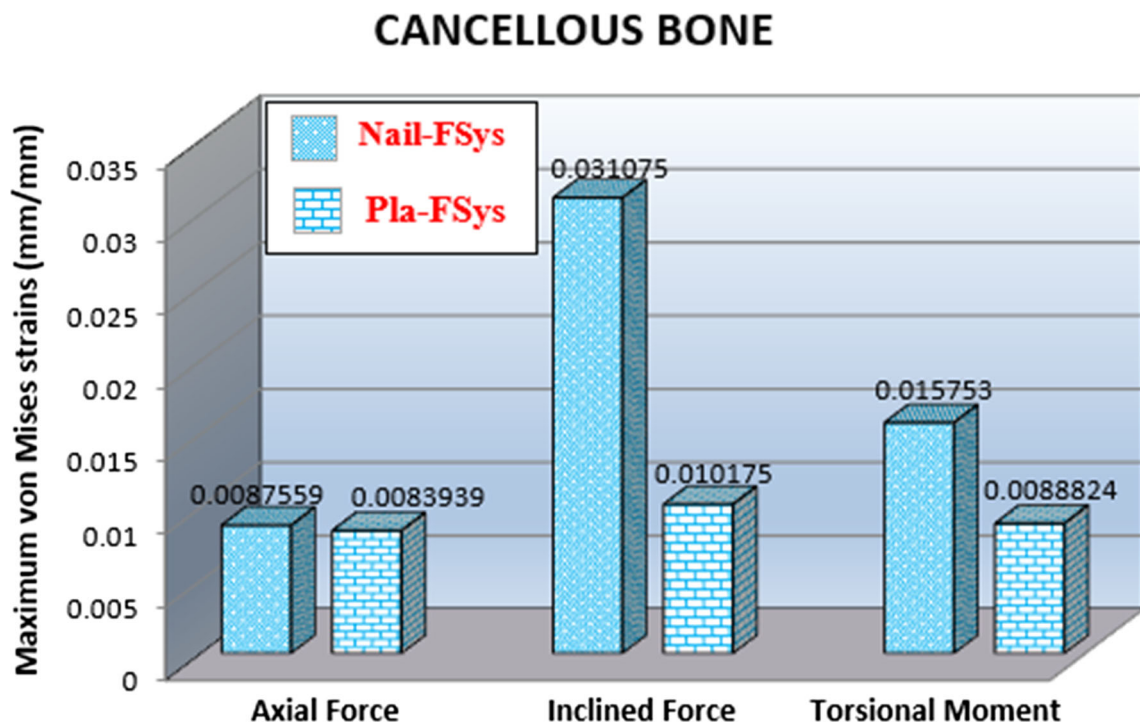
lower part of the humerus for Nail-FSys, and at the level of the medial humerus fracture for Pla-FSys.

Figure 15 shows the evolution of the maximum values of von Mises stresses in the cancellous bone of the fractured humerus using both fixation systems under the effect of different types of loadings. From this figure, we can observe that the system which generates more stress in the cancellous bone is that of intramedullary nailing. Indeed, in the case of a torsional moment, the maximum stress in the intramedullary nail fixation system is always higher than that in the plate fixation system. A slight difference was

observed between both systems for the case of axial force. The greatest difference was found in the case of inclined force, where it exceeds three times that generated by the compression plate system.

### Distribution of Strains in the Cancellous Bone

Figures 16 and 17 show, respectively, the strains distribution and the maximum values of strain in the cancellous bone of the fractured humerus using both fixation systems under the three types of loadings (axial force, inclined



**Fig. 17** Histogram of the maximum strains in the cancellous bone of the fractured humerus for both fixation systems (intramedullary nail and plate fixation system) under the effect of three types of loadings: (a) axial force, (b) inclined force and (c) torsional moment

force, and torque). The greatest strain is obtained when using the intramedullary nail fixation system under the effect of an inclined force loading, while the lowest strain is obtained in the case of axial force using the second fastening system. In addition, it can be noted that the maximum strains obtained in the case of the nailing fixation system are three times greater than those obtained by compression plate when the applied loads are inclined forces and are almost doubled for torsional moments (Fig. 16). A slight difference was found between both systems when the applied load was an axial force. In general, the histogram presented in Fig. 17 shows that the strain levels in the cancellous bone of the fractured humerus were reduced using the second fixation system (Pla-FSys) in the case of inclined force or torque loading.

#### Distribution of von Mises Stresses in Fixation Systems

Figure 18 shows the distribution of von Mises stresses in the intramedullary nail and the humeral fixation plate for different types of loads (axial force, inclined force, and torque). It can be noted that the highest stress level is obtained when using an intramedullary nail fixation system under the effect of an inclined force type loading, while the lowest stress level is recorded in the case of axial force using the same fixation system. Furthermore, the concentration of the maximum von Mises stresses is in the vicinity of the fracture for both surgical treatment systems.

Figure 19 shows the maximum values of the von Mises stresses for both fixation systems (intramedullary nail and plate fixation system) under the three types of loading. The nail fixation system generates the highest stresses. Indeed,

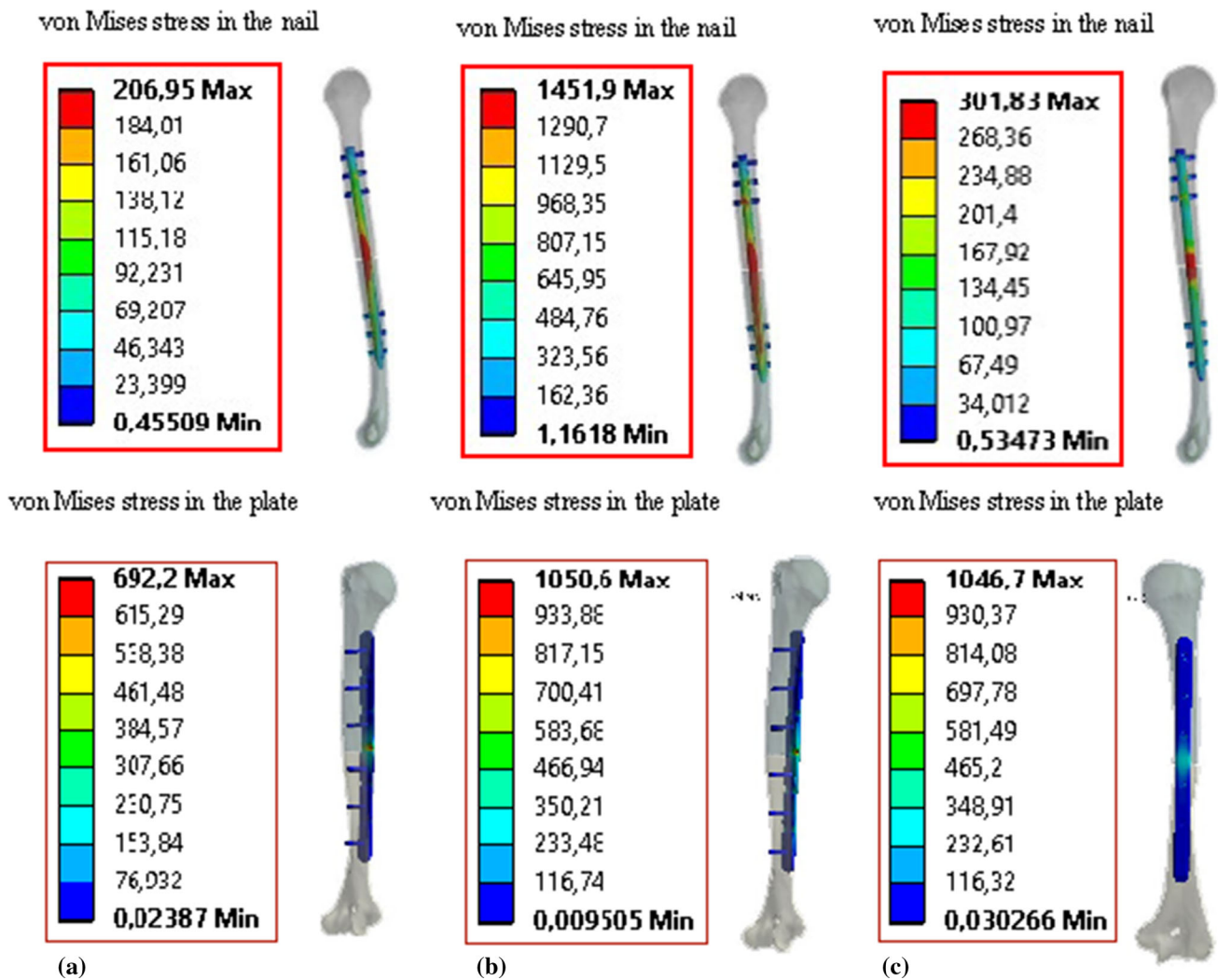


**Fig. 18** Von Mises stress distributions in the intramedullary nail and plate fixation system for different loads: (a) axial force, (b) shear force and (c) torque

in the case of axial force and torque, the maximum stress in the plate fixation system is more than three times higher than that obtained by nailing. However, in the case of torque, a slight difference has been found between both fixation systems.

#### Distribution of Normal and Shear Stresses in Fixation Systems

In this section, we present the results of the normal and shear stresses to verify the strength conditions for both fixation systems studied. Figure 20 illustrates the effect of axial loading applied to the upper surface of the humerus by generating maximum shear stresses at the nail and plate

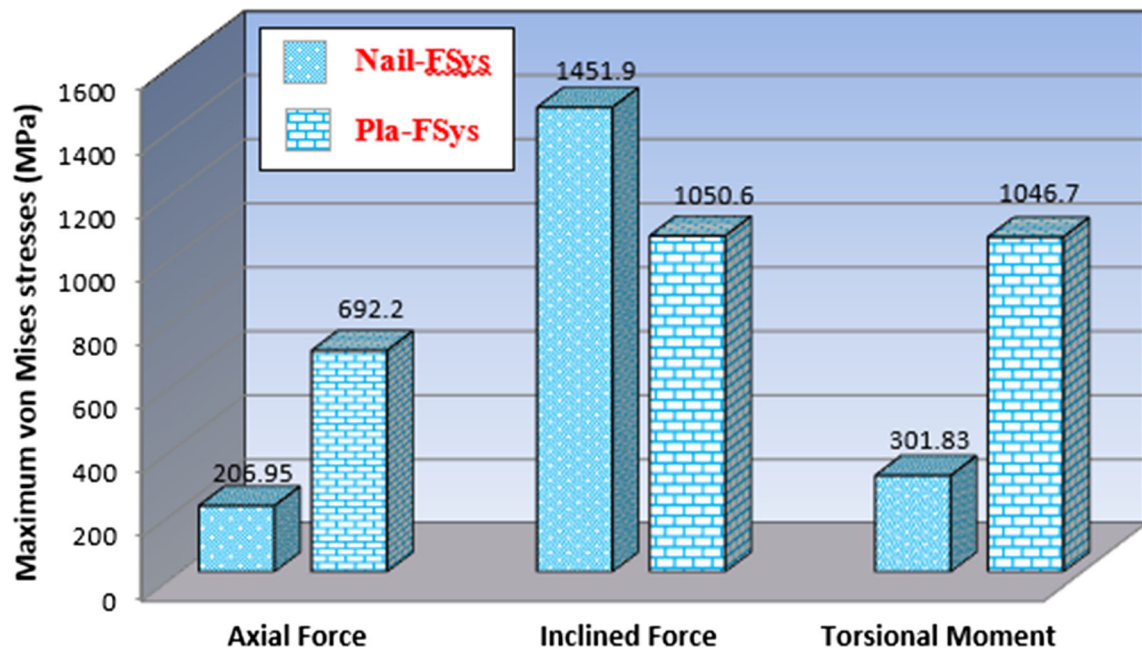
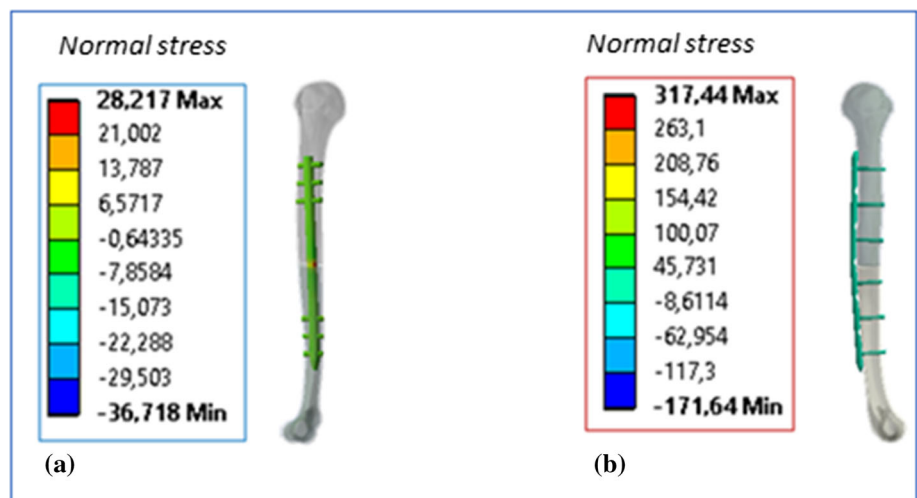


**Fig.19** Histogram of the maximum von Mises stresses at the level of both fixation systems (intramedullary nail and plate fixation system) for different types of loads: (axial force, inclined force, and torsional moment)

**Fig. 20** Distributions of normal stresses in (a) the intramedullary nail and (b) plate fixation system under the effect of axial force

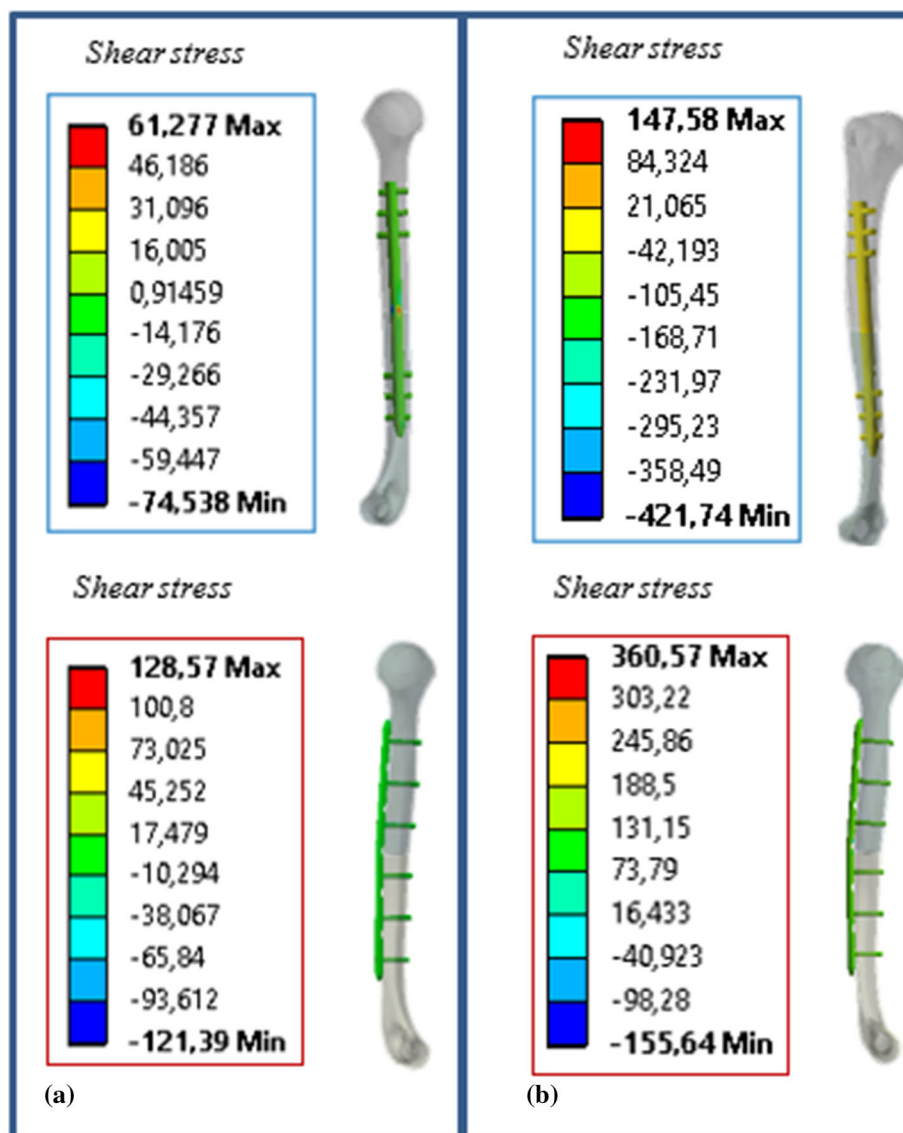


fixation system. It can be observed that the maximum values are, respectively, equal to 28.217 and 317.44 MPa (see red color is Fig. 20). In addition, we can notice that the strength condition is verified, as the maximum normal stresses in both fastening systems are lower than the

allowable compressive stress of the titanium alloy (Ti6Al4V) which is 970 MPa [25].

Figure 21a illustrates the effect of inclined load applied to the upper surface of the humerus generating shear stresses ranging from  $-74.538$  to  $61.277$  MPa at the level of the nailing stem and  $-121.39$  to  $128.57$  MPa for the plate

**Fig. 21** Distributions of shear stresses in the intramedullary nail and plate fixation system for the case of (a): shear force and (b): torque



fixation system. By comparing these values with the allowable shear stress of the titanium alloy (Ti6 Al4 V), which is equal to 550 MPa [25], we can confirm that the strength condition is verified.

Similarly, Fig. 21b shows the distribution of shear stresses in both fixation systems under a torsional torque of 10 Nm where their minimum and maximum values are,

respectively,  $-421.74$  and  $147.58$  MPa for the intramedullary nail and  $-155.64$  and  $360.57$  MPa for the plate fixation system. It can be easily noticed that the strength condition is verified since these values are always lower than the admissible value of the shear strength of the titanium alloy (Ti6Al4V), which is equal to 550 MPa.



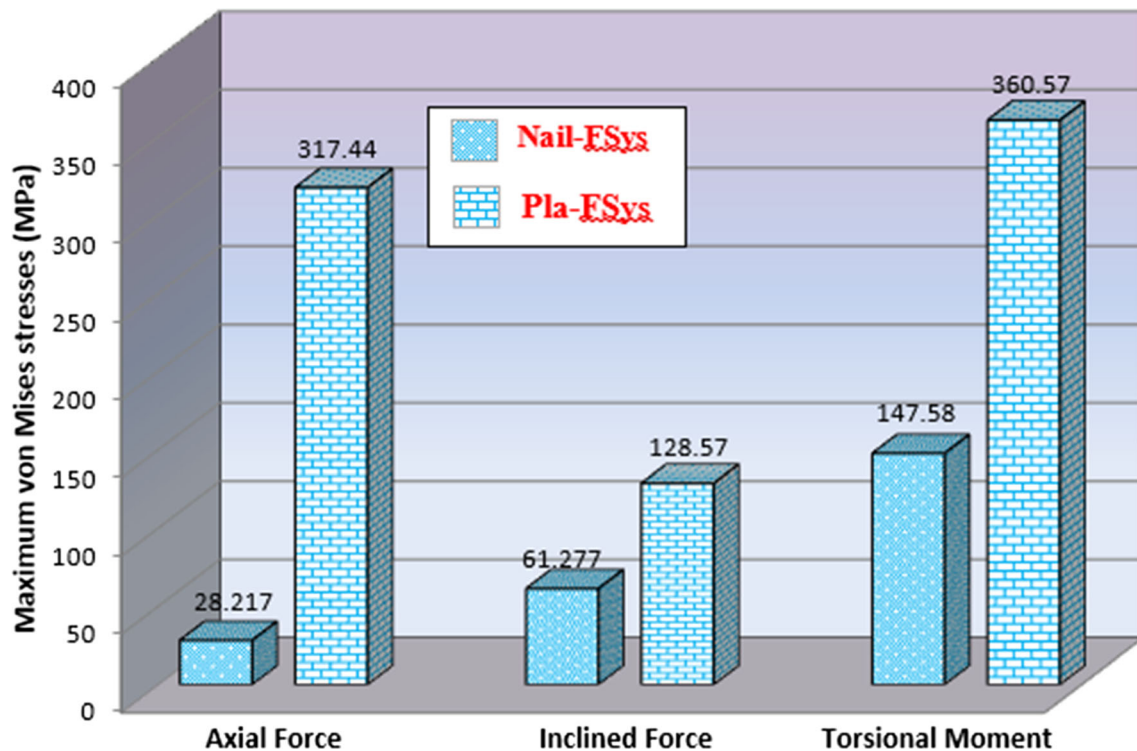


**Fig. 22** Histogram of maximum stresses in both fixation systems by intramedullary nailing (Nail-FSys) and plate fixation system (Pla-FSys)

Figure 22 summarizes the maximum values of normal stresses in the cases of axial force, inclined force and torsional moment for both fixation systems (Nail-FSys and Pla-FSys). It can be seen that for different types of loadings, the stresses generated in the plate fixation system (Pla-FSys) are always higher than those of the intramedullary nailing fixation system (Nail-FSys). Furthermore, the highest stresses are obtained in the case of plate fixation system when the applied load is an axial force (317.44 MPa) or a torsional torque (360.57 MPa). In general, the normal and shear stresses obtained in both fixation systems are always within the safety margin of the material used.

**Deformation of the Fixation Systems**

Figure 23 illustrates the distribution of strains in both fixation systems (Nail-FSys and Pla-FSys) under the effect of a torque of 10 Nm applied to the humeral head. It can be noted that the strain concentration is localized at the level

of the fractured zone of the humerus for both fixation systems. In fact, the strain in the plate fixation system is much greater than that of the intramedullary nail as their maximum values are, respectively, 0.0103 and 0.0021 (see Fig. 23). Therefore, it can be concluded that the nailing system is relatively more stable than that of the plate fixation system for the fixation of humeral fractures.

**Conclusions**

In this study, the finite element method was used to evaluate the equivalent stresses and strains in the fractured humerus fixed by intramedullary nailing and plate fixation system under the effect of three types of loadings (axial force, inclined force, and torque). From the results obtained, the following conclusions can be drawn:

- The stresses and strains in the cortical bone are always high compared to those in the cancellous bone for both

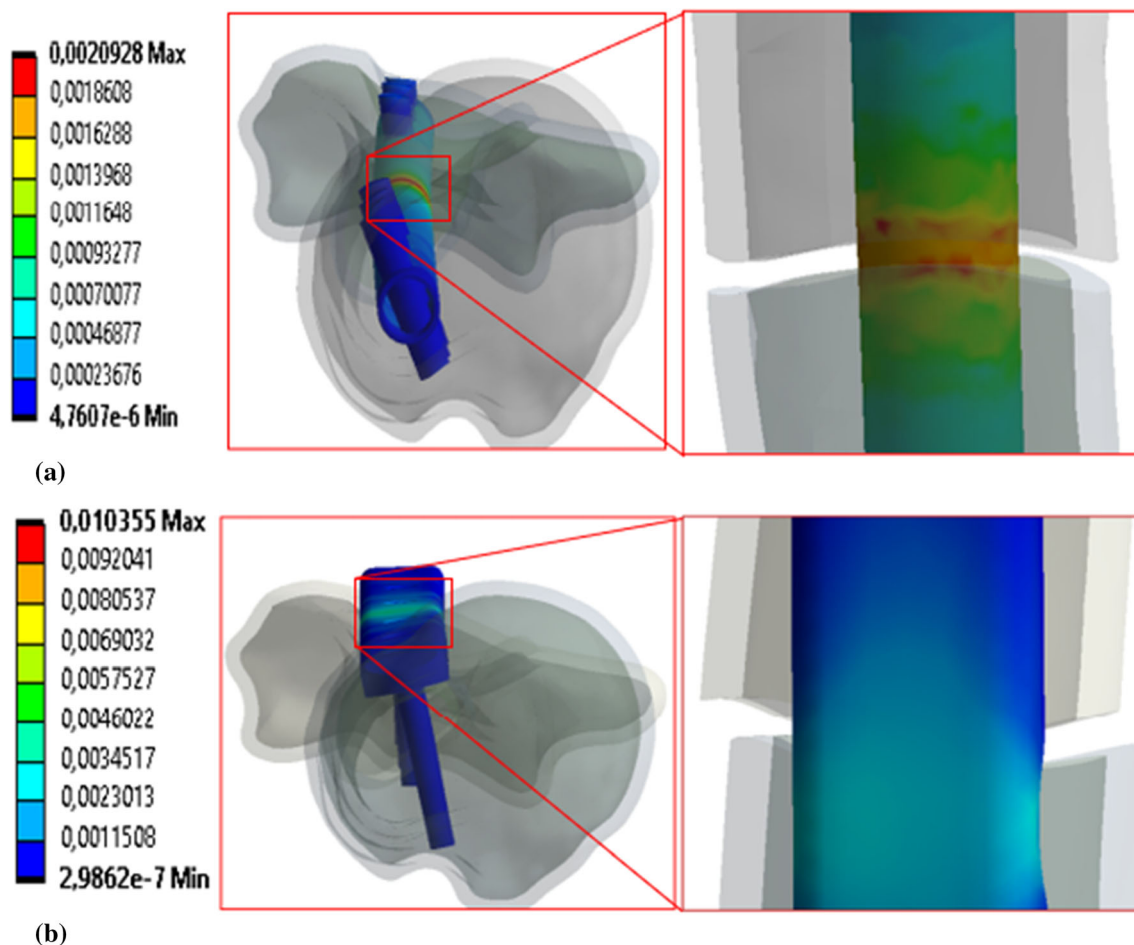


**Fig. 23** Distribution of equivalent strains in the case of angular torsion for both systems: **(a)**: intramedullary nailing (Nail-FSys) and **(b)**: plate fixation system (Pla-FSys)

fixation systems (intramedullary nail and plate surgical treatments)

- The lowest values of stresses and strains in both humeral bones (cortical and cancellous) and for both fixation systems are obtained in the case of axial loading, whereas the highest values are obtained in the case of inclined force.
- The von Mises, normal and shear stresses generated in the plate fixation system used for the surgical treatment of the humeral fracture are always higher than those found in the intramedullary nailing system.

In general, from the obtained results, it can be concluded that the use of the nailing fixation system (Nail-FSys) plays an important role in the reduction of stresses and strains in the fractured humerus compared to the plate fixation system (Pla-FSys).

In addition, it is important to note that the models developed in this work can provide a valuable numerical tool for the selection of the appropriate implants and the postoperative evaluation of surgical treatment.

## References

1. B.O. Sumrein, T.T. Huttunen, A.P. Lanonen, H.E. Berg, L. Felander-Tsai, V.M. Mattila, Proximal Humeral Fractures in Sweden—a Registry-Based Study. *Osteop. Int.* **28**, 901–907 (2017)
2. H.P. Dimas, A. Svedbom, A. Fahrleitner-Pammer, T. Pieber, H. Resch, E. Zwettler et al., Epidemiology of Proximal Humeral Fractures in Austria Between 1939 and 2008. *Osteop. Int.* **24**, 2413 (2013)
3. C. Rahrs, S. Tanja, B. Gunnar, B. Stig, A. Badke, S. Ulrich et al., Trends in Epidemiology and Patho-anatomical Pattern of Proximal Humeral Fractures. *Int. Orthop.* **38**, 1697–1704 (2014)
4. C.M. Court-Brown, B. Caesar, Epidemiology of Adult Fractures: a Review. *Injury.* **37**, 691–697 (2006)
5. N. Sudkamp, J. Bayer, P. Hepp, C. Voigt, H. Oestern, M. Kaab et al., Open Reduction and Internal Fixation of Proximal Humeral Fractures with use of the Locking Proximal Humerus Plate. Results of a Prospective, Multicenter, Observational Study. *J. Bone Joint Surg. Am.* **91**, 1320–1328 (2009)
6. F. Brunner, C. Sommer, C. Bahrs, R. Heuwinkel, C. Hafner, P. Rillmann et al., Open Reduction and Internal Fixation of Proximal Humerus Fractures Using a Proximal Humeral Locked plate: a Prospective Multicenter Analysis. *J. Orthop. Trauma.* **23**, 163–172 (2009)
7. G. Roderer, J. Erhardt, M. Kuster, P. Vegt, C. Bahrs, L. Kinzl et al., Second Generation Locked Plating of Proximal Humerus Fractures—a Prospective Multicenter Observational Study. *Int. Orthop.* **15**, 425–432 (2011)
8. B. Schliemann, I. Siemoneit, C. Theisen, C. Kusters, A. Weimann, M.J. Raschke, Complex Fractures of the Proximal Humerus in the Elderly—Outcome and Complication After Locking Plate Fixation. *Musculoskel Surg.* **96**, 3–11 (2012)
9. D. Krappinger, N. Bizzotto, S. Riedmann, C. Kammerlander, C. Hengg, F.S. Kralinger, Predicting Failure After Surgical Fixation of proximal Humerus Fractures. *Injury.* **42**, 1283–1288 (2011)
10. P.K. Zysset, E. Dall’ara, P. Varga, D.H. Pahr, Finite Element Analysis for Prediction of Bone Strength. *BoneKEY Rep.* **2**, 1–9 (2013)
11. A. Synek, Y. Chevalier, S.F. Baumbach, D.H. Pahr, The Influence a Bone Density and Anisotropy in Finite Element Models of Distal Radius Fracture Osteosynthesis: Evaluations and Comparison to Experiments. *J. Biomech.* **48**, 4116–4123 (2015)
12. Y.N. Chen, C.W. Chang, C.W. Iin, C.W. Wang, Y.T. Peng, C.H. Chang et al., Numerical Investigation of Fracture Impaction in Proximal Humeral Fracture Fixation with Locking Plate and Intramedullary Nail. *Int. Orthop.* **41**, 1471–1480 (2017)
13. Y. He, J. He, F. Wang, D. Zhou, Y. Wang, B. Wang et al., Application of Additional Medial Plate in Treatment of Proximal Humeral Fractures with Unstable Medial Column: a Finite Elements Study and Clinical Practice. *Medicine.* **94**(41), e1775 (2015)
14. P. Yang, Y. Zhang, Liu J., Xiao J., Ma LM., Zhu CR., Biomechanical Effect of Medial Cortical Support and Medial Screw Support on Locking Plate Fixation in Proximal Humeral Fractures with a Medial Gap: a Finite Element Analysis. *Acta Orthop. Traumatol. Turc.* **49**, 203–209 (2015)
15. J. Kennedy, E. Feerick, P. McGarry, D. FitzPatrick, H. Mullett, Effect of Calcium Triphosphate Cement on Proximal Humeral Fracture Osteosynthesis: a Finite Element Analysis. *J. Orthop. Surg.* **21**, 167–172 (2013)
16. F. Cukelj, J. Knezevic, J. Kodvanj, A. Bandalovic, M. Ostojic, K. Bilan et al., Computer Representation of Osteosynthesis Stability in Locking Plates Used for the Treatment of Osteoporotic Proximal Humerus Fractures. *Psychiatr. Danub.* **26**, 370–375 (2014)
17. P. Vargaa, J.A. Inzana, B. Gueorguiev, N.P. Südkamp, Windolf M., Validated Computational Framework for Efficient Systematic Evaluation of Osteoporotic Fracture Fixation in the Proximal Humerus. *Med. Eng. Phys.* **57**, 29–39 (2018)
18. P. Varga, I. Grunwald, J.A. Inzna, M. Windolf, Fatigue Failure of Plated Osteoporotic Proximal Humerus Fractures is Predicted by the Strain Around the Proximal Screws. *J Mech Behav Biomed Mater.* **75**, 68–74 (2017)
19. B. Keddar, B. Aour, S. Zahaf, (2019), Article: Static Study and Finite Element Analysis of a New Method of Fixation of a Medial Humerus Fracture by an Intramedullary Nailing System Analyzed by the ANSYS Workbench 16.2 Calculus Code. *Nano Biomed. Eng.* **11**(3), 272–289 (2019)
20. Y. He, Y. Zhang, Y. Wang, D. Zhou, F. Wang, Biomechanical Evaluation of a Novel Dual Plate Fixation Method for Proximal Humeral Fractures Without Medial Support. *J. Orthop. Surg. Res.* **12**, 72 (2017)
21. H. Sano, I. Wakabayashi, E. Itoi, Stress Distribution in the Supraspinatus Tendon with Partial-Thickness Tears: an Analysis Using Two-Dimensional Finite Element Model. *J. Shoulder Elbow Surg.* **15**, 100–105 (2006)
22. C. Masih, R. Nareliya, V. Kumar, In *Finite Element Application to Human Humerus Bone: A Biomechanical Study.* ed. by V. Kumar, M. Bhatele (2012) Proceedings of All India Seminar on Biomedical Engineering (AISOBE 2012) Lecture Notes in Bioengineering
23. L. Zhao, D. Tian, Y. Wei, J. Zhang, Z. Di, Z. He, Y. Hu, Biomechanical Analysis of a Novel Intercalary Prosthesis for Humeral Diaphyseal Segmental Defect Reconstruction. *Orthop. Surg.* **10**, 23–31 (2018)
24. Y. He, J. He, F. Wang, D. Zhou et al., Application of Additional Medial Plate in Treatment of Proximal Humeral Fractures with Unstable Medial Column: A Finite Element Study and Clinical Practice. *Medicine.* **94**(41), E1775–E1785 (2015)
25. M.H. John, Ed. Technical, C.Y. Ho (ed.), *Structural Alloys Handbook* (Cindas/Purdue University, West Lafayette, 1996)

**Publisher’s Note** Springer Nature remains neutral with regard to jurisdictional claims in published maps and institutional affiliations.